

## AUTOMATIC DETECTION OF TUMOR IN KIDNEY HARNESING IMAGE PROCESSING APPROACH

R.Lakshmana Kumar

Department of Computer Applications, Hindusthan College of Engineering and Technology ,Coimbatore,  
Tamilnadu,India.

E-mail: research.laksha@gmail.com

**Abstract**-Kidney cancer is regarded as the most common kind of cancer and lack of its early detection as well as quicker spread results in mortality. The fact that kidney tumours progress with little to no symptoms, unlike other cancer forms, is the driving force behind this research. This paper proposes an approach for detecting kidney tumors which uses a gaussian filter to compute the average weight of the neighbouring pixel points. Following that, the image is segmented utilizing Fuzzy C-means clustering for data segmentation by assigning a value to each pixel of the mage. Furthermore, feature extraction deploying Independent Component Analysis is enacted, which represents a group of random variables utilizing primary functions. Finally, the image is classified using Radial Basis Function Networks, which performs approximation of any normal function. This method uses a kidney tumor dataset and the accuracy obtained by RBF is 97% thus efficiently detecting the presence of tumor in kidney.

**Keywords:** Gaussian filter, Speckle noise, Fuzzy C- means, ICA, RBF.

### 1 INTRODUCTION

Kidney tumours may be benign or cancerous. The most common form of kidney cyst is benevolent and is distinct from tissue with cancer. It is common in the body, do not need to be treated unless they are causing symptoms[1]. Medical image processing is regarded as a valuable approach for the segmentation and detection of kidney tumors along with the reconstruction and interpretation of tumor images [2]. In most cases, the ideas behind the analysis of images are used to render an automated diagnosis based on the groups which are already described. Image intensity and texture differences occur as well, decreasing the contrast. Hence, the fragments are identified and the images are generally grouped, resulting in foliated attributes consuming lot of space resulting in increased convergence [3,4].

Considering these factors, images require four phases namely: preprocessing, segmentation, feature extraction and classification. Preprocessing begins with the speckle noise elimination, which prevents the loss of information about edges and important features. Various researches on reducing speckle noise were conducted over the past few decades. Linear filters are thought to be one of the most effective methods for image preprocessing in which its transfer function alters a part of the frequency spectrum of signal. But, they disregard the noise as well as image characteristics dispersed across the image, due to which the contrast as well as image's edge field is blurred [5, 6]. In this group, probabilistic nonlocal means filtering (PNLM) is a relatively new technique. Since average functioning is a primary criterion regarding procedures with spatial domain, the loss of increased information of frequency cannot be avoided [7]. Mathematical morphology (MM)

filtering methods use organisational windows with specific shapes to highlight structure features, which are referred to as structuring elements. Adaptive morphological operators are being built further in permitting the shaping structuring elements in which the shapes are flexible with the local features of the images processed. [8]. Another type of predefined filter is the Discrete Cosine Transform (DCT) filter, which is widely used in real-time applications to obtain input attributes with minimal time for reconstruction. Yet, these filters need to be improved in terms of efficiency and quality [9]. Considering the above-mentioned disadvantages, the gaussian filter is used in this approach for efficient image preprocessing by eliminating noise while computing average weights.

Following preprocessing, the images must be segmented, which is a vital step in both medical science and clinical practice. With the varying restrictions of illumination, manual image segmentation can help increase the efficiency of processing approaches[10]. Segmenting automatically is important since manual segmentation of three-dimensional images takes a long time and is subjected to inter-and intraobserver variance. Automatic Optic Disc (OD) and Optic Cup (OC) segmenting methods are considered as emerging approaches for segmentation . Contrast thresholding, color, level set approach, and techniques based on clustering were used in prior attempts at OC and OD segmentation. On the other hand, features which are manually designed lack sufficient discriminative ability, hence imaging circumstances and the intricateness of pathological regions have a major impact on performance [11].The technique of Atlas-based segmentation (ABS) is commonly known as well as commonly utilized for the extraction of contours from organ images. The images which are processed are saved in atlas collection in this

form[12]. As a result, the fuzzy C-means clustering algorithm is utilized in this method, which assigns individual value to every pixel of the image performing efficient segmentation.

Following image segmentation, feature extraction, a dimensionality reduction operation, is carried out. A relevant feature group is local feature descriptors. These local discriminative concepts were first created for multimedia image processing.[13, 14]. While extraction of features of multiple processes manage correlated as well as features with noise, the method is inappropriate for classification issues involving multi-modally featured images. Every feature is conjugated as a single vector but does not consider diversity of feature, results in serious "curse of dimensionality" [15]. Linear Discriminant Analysis (LDA) is another feature extraction method that aims to increase the gap between each class's mean as well as reduce class spread. However, it needed additional capability enhancements that provided limited side details, as well as rigidity against rotation and content loss attacks [16, 17]. Therefore, Independent Component Analysis (ICA) is adopted for extracting features avoiding redundant information.

Following image feature extraction, classification is to be performed which involves categorizing all pixels of digital image into one of many classes. Back propagation neural network (BPN) performs efficient classification of images but generate minimal accuracy with less detection speed [18, 19]. The Hopfield neural network is utilized for creating an improved classifier, with the matrix of pattern function. If a test weld's pattern feature matrix is fed, convergence into a state which is stable occurs, resulting in efficient classified results [20, 21]. A decision tree (DT) is another classification method for determining the most effective attribute component of classifying ability. The data is be partitioned into different subsets using the best attribute variables. Decision trees, in particular, are classification methods characterized by their improved interpretability and robustness. However, since the precision of integrated and sub-classifiers is strongly correlated, it is critical to develop classifiers that have higher classification accuracy [22]. Considering these drawbacks, Radial Basis Function Networks (RBF) are used for image classification, performing the approximation of any normal function.

In this paper, efficient detection of cancer in kidney is performed adopting image processing concepts. The contributions of the proposed approach are,

- The preprocessing of images is done by gaussian filter to reduce the speckle noise
- Fuzzy C-means clustering is adopted for segmentation by clustering approach.

- The necessary image features are extracted by ICA identifying optimal number of features.
- RBF is adopted for classification with improved accuracy.

The description is given by: Section 2 elucidates the related searches, section 3 demonstrates the proposed concept, section 4 includes the discussion about obtained results and section 5 includes conclusion.

## 2 RELATED WORKS

Aaron et al [23] developed a method for detecting the fluorescent property of agents which are contrast, specifically indocyanine green (ICG).The developed device underwent performance testing for optics and the detection of ICG presence in tumors as well as spontaneous tumors was analyzed.The highlight of this research was designing as well as testing a surgery device guided by image using a handheld source for excitation as well as spectrograph in conjunction with an imaging system.

Junquiang et al [24] adopted a method in which the results of a computed tomography (CT) scan of the kidney were examined and pathologically correlated.A total of ten tumor predicted cases were gathered as well as examined respectively.In six of the cases, the tumors were limited to the contour of kidney, with its enlarging. Several variations exhibiting nodules were discovered in these cases.

Wojciech et al [25] built a novel kidney segmentation algorithm that is completely automated. This method is intended for the study of vast databases containing both physiological and pathological events.This paper described the creation and application of a watershed transform which is controlled by 3D marker regarding segmentation of kidney images.The evolution of 3D marker images is automatic and is the first and most difficult phase in the current proposal.The labelled image analysis attained is the final kidney segmentation stage.

Nicole et al [26] examined the influence caused by utilizing 3D printed as well as virtual reality concepts for the awareness of patient towards the sense of renal as well as prostate cancer.Patients were randomised to obtain pre-operative preparation with separated imaging or other combined imaging concepts.

Margaret et al [27] illustrated the impact of renal models which are 3D printed and is physical in nature. The enhancement masses for characterization of medical trainee, localization, as well as comprehension of malignant renal tumor was studied.The processing of tumor images was performed along with its efficient classification generating the nature of tumor stages.

### 3 PROPOSED METHODOLOGY

The basic schematic process flow of the the processing of input images of kidney and its retrieval is given in figure 1. Initially, the input image of the kidney affected with tumor is fed to the gaussian filter for preprocessing, which generates an image free from speckle noise. This pre-processing of image does not affect its sharpness. The noise-free image is then segmented using Fuzzy C means clustering, which involves segmenting the data and generating a mean value for each cluster. Consequently, the reduction of computation time as well as memory utilization is performed by ICA with the extraction of features. Finally, the classification of image is performed by RBF, and the efficient detection of kidney tumor is performed.

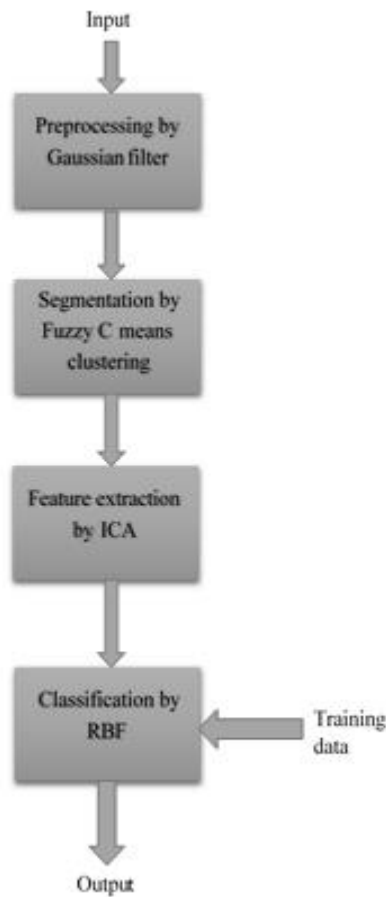


Figure 1 Proposed block diagram

#### 3.1 Image Preprocessing

Gaussian filter is adopted for the pre-processing of image which utilizes the smoothed cutoff process avoiding the truncation of coefficients of frequency. It

inherits the merits of discrete fourier transform and alters the components of frequency which are farther from the centre of the image.

Masks of odd sizes are used in Gaussian filtering. A value is computed for each point of the mask using a function that expresses the Gaussian distribution. The Gaussian function which is continuous is given by,

$$g(x) = \frac{1}{\sigma\sqrt{2\pi}} e^{-\left(\frac{y-\mu}{\sigma}\right)^2 \frac{1}{2}} \quad (1)$$

#### 3.2 Segmentation of Image

Following the pre-processing of image, the image segmentation has to be done by utilizing Fuzzy C means clustering approach. By assigning an individual value to every image pixel, fuzzy concept is used for processing data. Fuzzy set's membership value is between 0 and 1. Clustering is a form of unsupervised learning system. As a result, the segmentation methods based on it do not require training sample data; instead, they group pixels to form data clusters. Fuzzy clustering is a multi-valued logic system that employs intermediate values, which means that members of one fuzzy set may also be members of another fuzzy set in the same picture. Between full membership and nonmembership functions, there are no abrupt or discontinuous transitions. The membership role determines the fuzziness of an image as well as the details it contains. The core, support, and boundary features are the most important when using a membership function to characterise something. The fuzzy collection encompasses the entire core. The help is the set's non-membership value, while the boundary is the set's partial membership value, which ranges from 0 to 1. The membership of each data point corresponding to each cluster centre is determined by the distance between the cluster centre and the data point. The closer the data is to the cluster centre, the more likely it is to belong to the cluster centre. As a result, the total of each data point's membership must equal one.

The corresponding steps are given below.

Let  $A = \{a_1, a_2, \dots, a_n\}$  denote datapoints and  $B = \{b_1, b_2, \dots, b_n\}$  denote group of centers.

1) Choose randomly C cluster centers.

2) Estimate fuzzy membership utilizing,

$$\mu_{xy} = \frac{1}{\sum_{k=1}^C (d_{xy}/d_{xk})^{\frac{2}{m-1}}} \quad (2)$$

3) Estimate the fuzzy centre utilizing,

$$f_x = \frac{\sum_{y=1}^n (\mu_{xy})^m p_i}{\sum_{y=1}^n (\mu_{xy})^m}, \forall y = 1, 2, \dots, C \quad (3)$$

4) Repeat (2) and (3) until minimal value of the objective function is attained.

### 3.3 Feature Extraction

It denotes the process of reducing mapping of data which is of multidimension into a dimension space which is minimum, mandatory for retrieval of features. It is often considered as pattern detection and prediction. The feature data are actually quite important for classifying process; ICA is adopted in this approach for the feature extraction process minimizing the complexity.

The main concept of ICA deals with representing a group of variables which are random in nature utilizing primary functions. Consider  $n$  source data which are mutually independent and  $M = (m_1, m_2, \dots, m_n)^t$  indicate the form of matrix. Then,

$$P(M) = \prod_{i=1}^n P_i(m_i) \quad (1)$$

The  $n$  number of data observed with the representation of matrix  $Y = (y_1, y_2, \dots, y_n)^t$ . Consider the data observed as linearly combined source data.

$$y_i = \sum_{j=1}^n a_{ij} m_j, i = 1, 2, \dots, n \quad (3)$$

And the representation of matrix is given by,

$$Y = AM \quad (4)$$

Here,  $A \rightarrow$  mixture matrix comprising of mixture coefficients.

The main objective of ICA is to identify a linear transformation given by  $W$  which has the ability to perform linear transformation of  $Y$  to  $X = (x_1, x_2, \dots, x_n)^t$  with mutually independent vectors. The matrix is denoted by,

$$X = AY \quad (5)$$

In which  $X$  indicates the source data estimation.

### 3.4 Classification of Images

Following feature extraction, image classification is carried out, which is a significant area in which deep neural networks are considered to be an essential factor in processing of medical image. To assess the existence of disease, the classification of image recognizes input images and produces a classified output image. Hence, an efficient RBF architecture is proposed in this approach which is shown in figure 2.

RBF comprises of three layers named as input, hidden as well as output layers. RBF is utilized broadly owing to its property of approximating any function

which is regular and possess improved speed for training. When the classification of pattern is needed, a sigmoid is located on the result for conveying output values as well as groups. The measure of distance is performed non-linearly which influences the value assigned. Generally, the measured distance is Euclidean value and for every neuron present in hidden layer, the centre coordinates are represented by the weights.

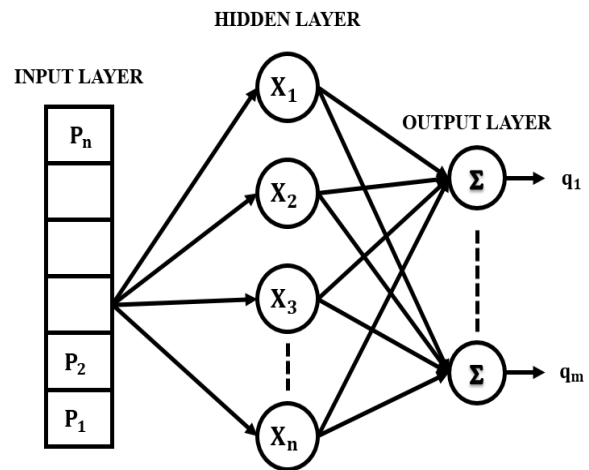
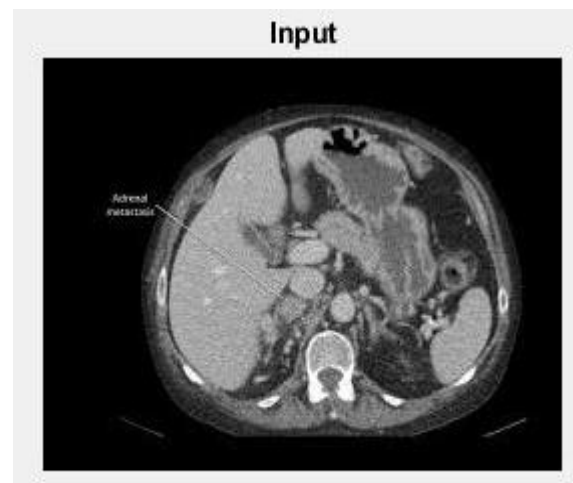


Figure 2 Architecture of RBF

## 4 RESULTS AND DISCUSSION

Kidney tumor dataset [28] is utilized for input images and the image resolution is  $510 \times 510$  of  $1 \times 1 \text{ mm}^2$  /pixel as well as the value of spacing is 1 mm. The dataset is classified into subsets named as training, validation as well as testing.



(a) Input image



(b) Gaussian filtered image

**Figure 3** Output of Gaussian filter

Figure 3 indicates the image filtered by median filter which is less noisy and has abundant data, hence making it appropriate for the purpose of diagnosis by physicians.

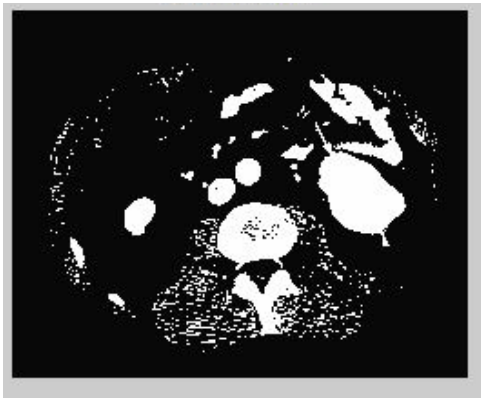


**Figure 4** Segmented output image by Fuzzy C-means clustering

Figure 4 indicates the segmented image in which the tumor affected region is clearly indicated. The segmentation adopting Fuzzy C-means clustering generated improved results compared to existing ones.

**Table 1** Comparison of methods with ICA and without ICA

|             | Without ICA | With ICA |
|-------------|-------------|----------|
| Accuracy    | 0.85        | 0.95     |
| Sensitivity | 0.62        | 0.75     |
| Specificity | 0.87        | 0.97     |

The table 1 indicates the comparison of efficiency of approaches adopting and non-adopting ICA. With the help of ICA, the values of accuracy, sensitivity as well as specificity showed improved results.

The outputs are estimated based on the performance measure parameters like True Positive (TP), True Negative (TN), False Positive (FP) and False Negative (FN) from which sensitivity, accuracy, and specificity values are calculated.

#### 4.1 Performance metrics

The performance analysis for the below mentioned metrics are done in this approach.

##### 4.1.1 Accuracy

It denotes the percentage of appropriately classified instances and is given by,

$$\text{Accuracy} = \frac{TP+TN}{TP+TN+FP+FN}$$

##### 4.1.2 Sensitivity

It denotes the proportion of positives that are accurately detected and is given by,

$$\text{Sensitivity} = \frac{TP}{TP+FN}$$

##### 4.1.3 Specificity

It denotes the proportion of negatives which are accurately detected and is given by,

$$\text{Specificity} = \frac{TN}{TN+FP}$$

Where TP → True Positive  
 TN → True Negative  
 FP → False Positive  
 FN → False Negative

##### 4.1.4 F-score

It denotes the measure of accuracy of tests performed and is given by

$$\text{F-measure} = \frac{(2 * \text{Precision} * \text{Recall})}{(\text{Precision} + \text{Recall})}$$

**Table 2** Comparison of RBF with existing methods

| Methods  | Accuracy | Sensitivity | Specificity | F-score |
|----------|----------|-------------|-------------|---------|
| BPN      | 91.0     | 90.9        | 90.91       | 0.9     |
| Hopfield | 91.0     | 90.0        | 91.0        | 0.91    |
| RBF      | 97.0     | 100         | 95.4        | 0.98    |

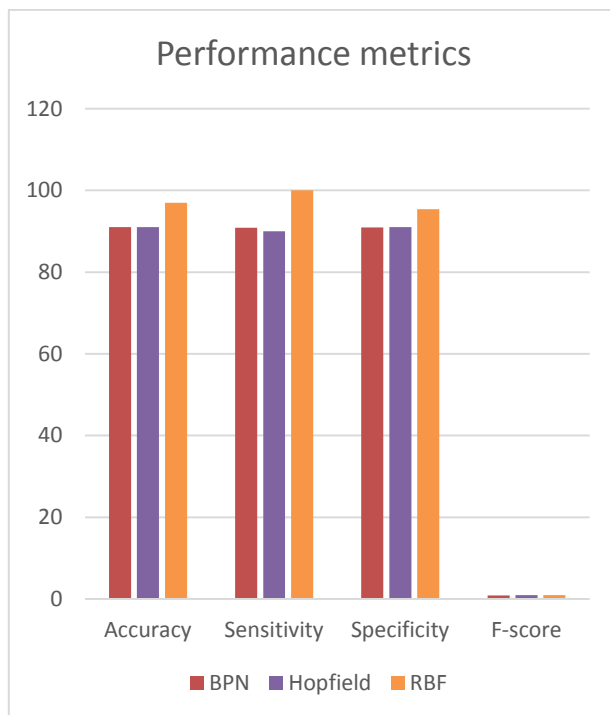


**Figure 5** Comparison of performance metrics

The table 2 indicates the comparison of overall accuracy values of RBF classifier with other classification approaches like BPN [29] and Hopfield[30] and the corresponding characteristic plot for accuracy is shown in figure 5.

Thus the efficient kidney tumor detection is performed through image processing concepts like preprocessing, segmentation, feature extraction as well as classification of images.

## 5 CONCLUSION

In this paper, basic concepts of image processing are applied to the images of kidney. The speckle noise is eliminated by the gaussian filter and the pre-processed image is segmented by Fuzzy C-means clustering approach. ICA is utilized for feature extraction process for obtaining the optimal set of features. The selected features are fed to the RBF for efficient classification of images. With RBF, excellent results are

obtained with overall accuracy of 97% along with improved prediction performance. The performance metrics including accuracy, sensitivity, specificity and F-score are analyzed. In future, classification performance can be enhanced with the application of optimization approaches.

## References

- [1] Tuncer, Seda Arslan, and Ahmet Alkan, "A decision support system for detection of the renal cell cancer in the kidney", *Measurement*, Vol. 123, pp. 298-303, 2018.
- [2] Kline, T. L., Korfiatis, P., Edwards, M. E., Blais, J. D., Czerwiec, F. S., Harris, P. C., & Erickson, B. J., "Performance of an artificial multi-observer deep neural network for fully automated segmentation of polycystic kidneys", *Journal of digital imaging*, Vol.30, no. 4, pp. 442-448, 2017.
- [3] Raju, Paladugu, VeeraMalleswaraRao, and BhimaPrabhakaraRao, "Optimal GLCM combined FCM segmentation algorithm for detection of kidney cysts and tumor", *Multimedia Tools and Applications*, Vol.78, no.13, pp. 18419-18441, 2019.
- [4] Jie Song, Liang Xiao, ZhichaoLian, "Contour-Seed Pairs Learning-Based Framework for Simultaneously Detecting and Segmenting Various Overlapping Cells/Nuclei in Microscopy Images", *IEEE Transactions on Image Processing*, Vol. 27, no. 12, pp. 5759 – 5774, 2018.
- [5] Hyunho Choi, JechangJeong, "Despeckling Images Using a Preprocessing Filter and Discrete Wavelet Transform-Based Noise Reduction Techniques", *IEEE Sensors Journal*, Vol. 18, no. 8, pp. 3131 – 3139, 2018.
- [6] Uzun, S., &Akgün, D, "An accelerated method for determining the weights of quadratic image filters", *IEEE Access*, Vol.6, pp. 33718-33726, 2018.
- [7] Balasubramanian Gopalan,A. Chilambuchelvan,S. Vijayan,G. Gowrison, "Performance Improvement of Average Based Spatial Filters through Multilevel Preprocessing using Wavelets", *IEEE Signal Processing Letters*, Vol. 22, No. 10, pp. 1698 – 1702, 2015.
- [8] Yidan Teng;Ye Zhang;Yushi Chen;Chunli Ti, "Adaptive Morphological Filtering Method for Structural Fusion Restoration of Hyperspectral Images", *IEEE Journal of Selected Topics in Applied Earth Observations and Remote Sensing*, Vol. 9, No. 2, pp. 655 – 667, 2016.
- [9] Lawgaly, Ashref, and Fouad Khelifi, "Sensor pattern noise estimation based on improved locally adaptive DCT filtering and weighted averaging for source

- camera identification and verification", IEEE Transactions on Information Forensics and Security, Vol. 12, no. 2, pp. 392-404, 2016.
- [10] Subhamoy Mandal;Xosé Luís Deán-Ben;Daniel Razansky, "Visual Quality Enhancement in Optoacoustic Tomography Using Active Contour Segmentation Priors", IEEE Transactions on Medical Imaging, Vol. 35, No. 10, pp. 2209 – 2217, 2016.
- [11] Fu, H., Cheng, J., Xu, Y., Wong, D. W. K., Liu, J., & Cao, X, "Joint optic disc and cup segmentation based on multi-label deep network and polar transformation", IEEE transactions on medical imaging, Vol.37, no.7, pp. 1597-1605, 2018.
- [12] Farzad Khalvati;Cristina Gallego-Ortiz;Sharmila Balasingham;Anne L. Martel, "Automated Segmentation of Breast in 3-D MR Images Using a Robust Atlas", IEEE Transactions on Medical Imaging, Vol. 34, No. 1, pp. 116 – 125, 2015.
- [13] Florin-Andrei Georgescu;Corina Vaduva;Dan Raducanu;Mihai Datcu, "Feature Extraction for Patch-Based Classification of Multispectral Earth Observation Images", IEEE Geoscience and Remote Sensing Letters, Vol. 13, No. 6, pp. 865 – 869, 2016.
- [14] Xia, Z., Ma, X., Shen, Z., Sun, X., Xiong, N. N., & Jeon, B, "Secure image LBP feature extraction in cloud-based smart campus", IEEE Access, Vol. 6, pp. 30392-30401, 2018.
- [15] Yong Luo;Yonggang Wen;Dacheng Tao;Jie Gui;Chao Xu, "Large Margin Multi-Modal Multi-Task Feature Extraction for Image Classification", IEEE Transactions on Image Processing, Vol. 25, No. 1, pp. 414 – 427, 2016.
- [16] Xiang Zhang, Fei Peng, Min Long, "Robust Coverless Image Steganography Based on DCT and LDA Topic Classification", IEEE Transactions on Multimedia, Vol. 20, no. 12, pp. 3223 – 3238, 2018.
- [17] Ye, Qiaolin, Henghao Zhao, Liyong Fu, and Shanbing Gao, "Underlying connections between algorithms for nongreedy LDA-L1", IEEE Transactions on Image Processing, Vol. 27, no. 5, pp. 2557-2559, 2018.
- [18] Chiba, Zouhair, Nouredine Abghour, Khalid Moussaid, and M. Rida. "A cooperative and hybrid network intrusion detection framework in cloud computing based on snort and optimized back propagation neural network", Procedia Computer Science, Vol. 83, pp. 1200-1206, 2016.
- [19] Mala, K., V. Sadasivam, and S. Alagappan, "Neural network based texture analysis of CT images for fatty and cirrhosis liver classification." Applied Soft Computing, Vol. 32, pp.80-86, 2015.
- [20] Jayashree, J., and S. Ananda Kumar. "Evolutionary correlated gravitational search algorithm (ECGS) with genetic optimized Hopfield neural network (GHNN)—A hybrid expert system for diagnosis of diabetes", Measurement, Vol. 145, pp. 551-558, 2019.
- [21] Hemanth, D. Jude, J. Anitha, and Mamta Mittal. "Diabetic retinopathy diagnosis from retinal images using modified hopfield neural network", Journal of medical systems, Vol.42, No. 12, pp. 1-6, 2018.
- [22] Rafael Rivera-Lopez, Juana Canul-Reich, "Construction of Near-Optimal Axis-Parallel Decision Trees Using a Differential-Evolution-Based Approach", IEEE Access, Vol. 6, pp. 5548 – 5563, 2018.
- [23] Aaron M. Mohs, Michael C. Mancini, James M. Provenzale, Corey F. Saba, Karen K. Cornell, Elizabeth W. Howerth, Shuming Nie, "An Integrated Widefield Imaging and Spectroscopy System for Contrast-Enhanced, Image-Guided Resection of Tumors", IEEE Transactions on Biomedical Engineering, Vol. 62, No. 5, pp. 1416 – 1424, 2015.
- [24] Dong, Junqiang, Jingjing Xing, Hangsha Hang Limbu, Songwei Yue, Lei Su, Dandan Zhang, and Jianbo Gao. "CT features and pathological correlation of primitive neuroectodermal tumor of the kidney." Cell biochemistry and biophysics, Vol. 73, No. 1, pp. 59-64, 2015.
- [25] Wieclawek, Wojciech. "3D marker-controlled watershed for kidney segmentation in clinical CT exams", Biomedical engineering online, Vol. 17, No. 1, pp.1-21, 2018.
- [26] Wake, Nicole, Andrew B. Rosenkrantz, Richard Huang, Katalina U. Park, James S. Wysock, Samir S. Taneja, William C. Huang, Daniel K. Sodickson, and Hersh Chandarana. "Patient-specific 3D printed and augmented reality kidney and prostate cancer models: impact on patient education", 3D printing in medicine, Vol. 5, No. 1, pp.1-8, 2019.
- [27] Marsh, J. N., Matlock, M. K., Kudose, S., Liu, T. C., Stappenbeck, T. S., Gaut, J. P., & Swamidass, S. J, "Deep learning global glomerulosclerosis in transplant kidney frozen sections", IEEE transactions on medical imaging, Vol. 37, no. 12, pp. 2718-2728, 2018.
- [28] Knoedler, Margaret, Allison H. Feibus, Andrew Lange, Michael M. Maddox, Elisa Ledet, Raju Thomas, and Jonathan L. Silberstein. "Individualized physical 3-dimensional kidney tumor models constructed from 3-dimensional printers result in improved trainee anatomic understanding", Urology, Vol. 85, No. 6, pp.1257-1262, 2015.
- [29] Latif, G., Iskandar, D. A., Alghazo, J. M., & Mohammad, N, "Enhanced MR image classification using hybrid statistical and wavelets

- features”, IEEE Access, Vol.7, pp. 9634-9644, 2018.
- [30] Devkota, B., Alsadoon, A., Prasad, P. W. C., Singh, A. K., & Elchouemi, A, “Image segmentation for early stage brain tumor detection using mathematical morphological reconstruction”, Procedia Computer Science, Vol.125, pp. 115-123, 2018.